

Improving Handwritten Text Recognition via 3D Attention and Multi-Scale Training

Zi-Rui Wang

Chongqing, China

Abstract. The segmentation-free research efforts for addressing handwritten text recognition can be divided into three categories: connectionist temporal classification (CTC), hidden Markov model and encoder-decoder methods. In this paper, inspired by the above three modeling methods, we propose a new recognition network by using a novel three-dimensional (3D) attention module and global-local context information. Based on the feature maps of the last convolutional layer, a series of 3D blocks with different resolutions are split. Then, these 3D blocks are fed into the 3D attention module to generate sequential visual features. Finally, by integrating the visual features and the corresponding global-local context features, a well-designed representation can be obtained. Main canonical neural units including attention mechanisms, fully-connected layer, recurrent unit and convolutional layer are efficiently organized into a network and can be jointly trained by the CTC loss and the cross-entropy loss. Experiments on the latest Chinese handwritten text datasets (the SCUT-HCCDoc and the SCUT-EPT) and one English handwritten text dataset (the IAM) show that the proposed method can achieve comparable results with the state-of-the-art methods. The code is available at <https://github.com/Wukong90/3DAttention-MultiScaleTraining-for-HTR>.

Keywords: Handwritten text recognition · Segmentation-free recognition · 3D attention module · Multi-scale training · Global-local context information.

1 Introduction

There are three typical segmentation-free methods, i.e., hidden Markov model (HMM) [1, 2], connectionist temporal classification (CTC)[3–8] and encoder-decoder (ED) framework [9–12]. As shown in Fig. 1, in the HMM-based method, each character is modeled by an HMM and a text line can be represented by cascaded HMMs. A series of frames extracted from an original image by a left-to-right sliding window are assigned to the underlying states. Then, a neural network is used to estimate the posterior probabilities of the states, while the outputs of networks in CTC and ED-based approaches are character classes. In the CTC loss, a special character "blank" and a sophisticated rule are designed to split different characters, and the forward-backward algorithm can efficiently compute

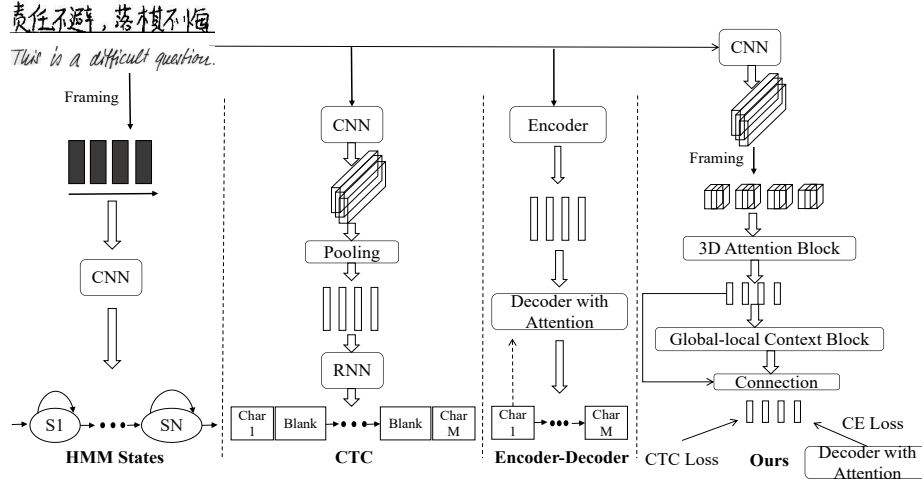


Fig. 1. The typical segmentation-free methods and the proposed network. The abbreviations CNN, RNN, Char, S denote convolutional neural network, recurrent neural network, character and state, respectively.

the probability of the underlying character sequence. In an encoder-decoder network, an image is usually fed into the encoder to generate the corresponding middle features. Based on the middle representations, the decoder is used to locate and predict the character sequence via attention mechanisms. The common cross-entropy loss can be directly used to adjust the parameters of the ED network.

It is reasonable to explicitly model the 2D information of characters. However, it is very difficult to expand 1D HMM to 2D HMM [13] due to the computational complexity. Even for the CTC, ED-based approaches [14, 15, 6, 10], early networks just simply depend on the local receptive field of convolutional layers or recurrent units and gradually shrink the height of feature maps to small pixels via stacked pooling layers, which may lead to information loss. Although some attempts [16, 17, 11, 18] explicitly or implicitly employ 2D information in scene text recognition and character recognition, there is no obviously evidence shows that these method can be directly used in long handwritten text recognition. Obviously, the context information is important for the text recognition. In [19–21], the visual features and the linguistic knowledge are simultaneously integrated into a network. Actually, based on the visual features extracted from a certain image, the corresponding context information can also be naturally obtained by using recurrent units [5, 16, 22, 8] or transformers [17, 23, 24].

For the handwritten text recognition task, recently, Hoang et al. [7] combined the radical-level CTC loss and the character-level loss while Ngo et al. [12] constructed a joint decoder to integrate the visual feature and the linguistic context feature. More recently, Peng et al. [25] built a full convolution network to simultaneously achieve the purpose of the character location, the character bounding

boxes prediction and the character prediction. Lin et al. [26] propose a mobile text recognizer via searching the lightweight neural units. Furthermore, Peng et al. [27] detect and recognize characters in page-level handwritten text while Coquenet et al. [23] employ a fully convolutional network as the encoder with a transformer decoder for document recognition.

In this paper, inspired by the above three modeling ways, we propose a new recognition network by using a novel 3D attention module and global-local context information. The 3D attention module is employed to explicitly extract 2D information of block features with different resolutions. In detail, the 3D attention module is ingeniously decoupled into a 2D self-attention operation and a 1D attention-based aggregation operation. Based on the outputs (visual features) of the 3D attention module, we further extract the corresponding global-local context information via the self-attention and the recurrent unit, respectively. Finally, by integrating the visual features and the corresponding global-local context features, a well-designed representation for the recognition task can be obtained. In summary, the main contributions of this paper are as follows:

1. Inspired by the typical segmentation-free approaches, we improve the text recognition network by using a novel 3D attention module and global-local context information.
2. Main canonical neural units including attention mechanisms, fully-connected layer, recurrent unit and convolutional layer are ingeniously organized into a network.
3. We propose the multi-scale training approach that includes extracting 3D blocks with different resolutions and simultaneously adopting the CTC and the CE losses.
4. Compared with the state-of-the-art methods, the proposed network can achieve comparable results on all datasets. We conduct a comprehensive analysis to verify the effects of the 3D attention module and the different features.

The remainder of this paper is organized as follows: Section 2 elaborates on the details of the proposed method. Section 3 reports the experimental results and analysis. Finally, we conclude the paper.

2 Methodology

As shown in Fig. 2, the proposed network includes three parts, i.e., the convolutional neural network (CNN), the 3D attention module and the features integration block. In the CNN, the hybrid attention module (HAM) [8] is used and each convolutional layer is equipped with the batch normalization [28]. For the outputs of the CNN, we employ a multi-scale framing strategy to extract different solutions. In this section, we elaborate on the details of the 3D attention module and the global-local context information. Moreover, the multi-scale training pipeline is also shown.

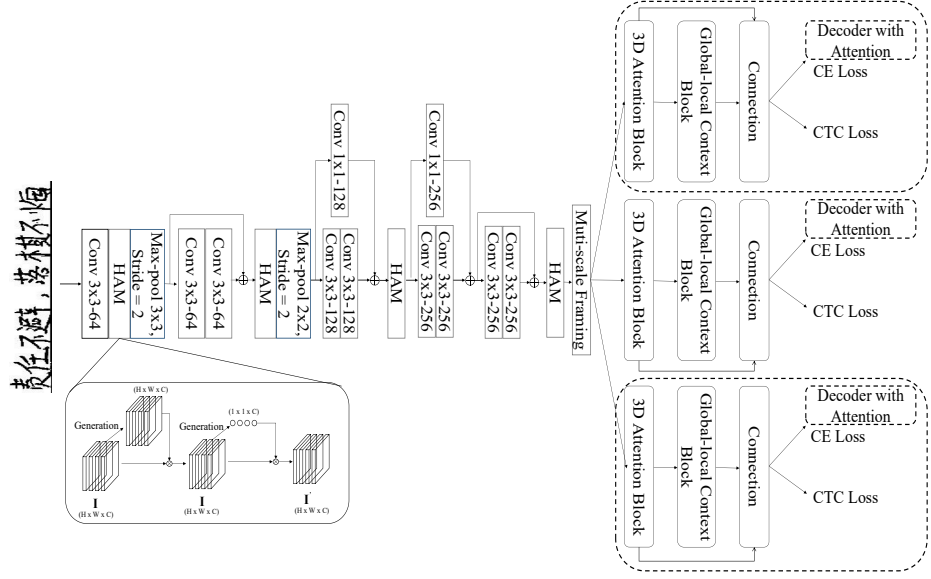


Fig. 2. The parts within the dashed lines are only used during the training stage. The details of the 3D attention, global-local context, decoder with attention, CE loss and CTC loss are illustrated in the following sections.

2.1 3D Attention

As shown in Fig. 3, assuming the front CNN has the output tensor $\mathbf{O} \in R^{C \times W \times H}$ with each feature map $\mathbf{O}_c \in R^{W \times H}$, each 3D block represented by a sliding window $\mathbf{f} \in R^{C \times S \times H}$ from left to right, with the window shift of S pixels, is scanned across the feature maps. Firstly, each location p in the plane $S \times H$ is added the corresponding positional encoding:

$$\mathbf{f}_p[0 : C/2] = \mathbf{f}_p[0 : C/2] + \mathbf{p}_w \quad (1)$$

$$\mathbf{f}_p[C/2 : (C - 1)] = \mathbf{f}_p[C/2 : (C - 1)] + \mathbf{p}_h \quad (2)$$

where \mathbf{p}_w and \mathbf{p}_h are sinusoidal positional encoding over height and width, respectively, as defined in [29]:

$$\mathbf{p}_{p,2i} = \sin(p * e^{2i * (-\ln(10000)/C)}) \quad (3)$$

$$\mathbf{p}_{p,2i+1} = \cos(p * e^{2i * (-\ln(10000)/C)}) \quad (4)$$

where i is indice along hidden dimensions. And then, we reshape each 3D block from $C \times S \times H$ to $SH \times C$ and conduct a self-attention operation for these sequential vectors \mathbf{f}_p as Eq.5:

$$\mathbf{F}' = \text{softmax}\left(\frac{\mathbf{F}\mathbf{F}^T}{s}\right)\mathbf{F} \quad (5)$$

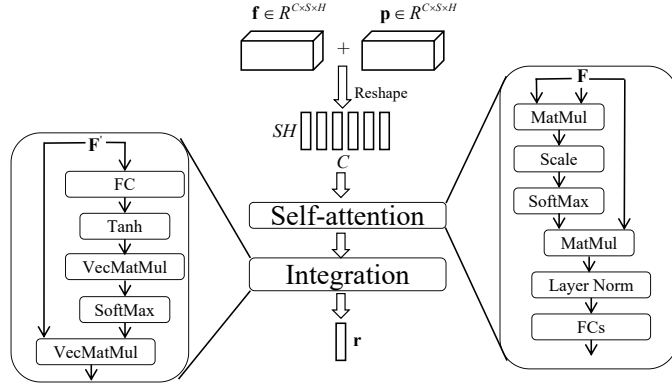


Fig. 3. The proposed 3D attention block.

The matrices \mathbf{F} , \mathbf{F}' pack all vectors \mathbf{f}_p and the corresponding \mathbf{f}'_p , respectively. Finally, a representation vector \mathbf{r} for all \mathbf{f}'_p can be obtained:

$$e_p = \mathbf{w}^T \tanh(\mathbf{W}\mathbf{f}'_p + \mathbf{b}) \quad (6)$$

$$\alpha_p = \frac{e_p}{\sum_i e_i} \quad (7)$$

$$\mathbf{r} = \sum_p \alpha_p \mathbf{f}'_p \quad (8)$$

Similar to the transformer encoder, the vectors \mathbf{f}'_p are fed into a layer normalization (Layer Norm) followed by two fully connected layers (FCs) before computing Eq.6-8.

2.2 Features Integration

Through the 3D attention module, a series of 3D feature maps can be transformed into the corresponding visual features $\mathbf{r}_t (t = 0 \dots T)$. As shown in Fig. 4-(a), for the visual feature \mathbf{r}_t , the global context feature \mathbf{l}_t and the local context \mathbf{s}_t can be extracted by using the self-attention mechanism and the recurrent units, respectively. In this paper, we directly employ the computation method of the \mathbf{f}' in Fig. 3 to obtain the global context information \mathbf{l}_t . For the local context features, the standard LSTM (Fig. 4-(b)) is used. \mathbf{r}_t represents the input at time t and \mathbf{s}_t is the corresponding output, \mathbf{i} , \mathbf{g} , \mathbf{o} and \mathbf{c} are the outputs of input gate, forget gate, output gate and cell vectors, respectively. Finally, the visual feature \mathbf{r}_t , the global feature \mathbf{l}_t and the local feature \mathbf{s}_t are simply contacted together:

$$\mathbf{v}_t = \mathbf{r}_t \oplus \mathbf{l}_t \oplus \mathbf{s}_t \quad (9)$$

The well-defined representations \mathbf{v} can be directly fed into a classification layer and also be used as the input of the decoder during the joint training of the CTC and the CE losses.

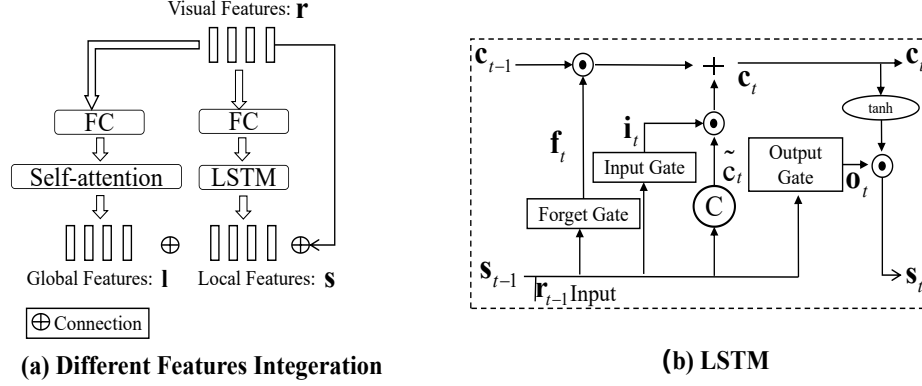


Fig. 4. The different features (visual features, global-local features) are combined before the classify layer and the details of the LSTM are illustrated.

2.3 Multi-Scale Training

The proposed multi-scale training include two parts. Firstly, as shown in Fig. 2, in the training stage, multiple feature sequences with different frame lengths are extracted. Although parallel branches including the same 3D attention block and global-local context block are used, we only retained the corresponding branch of the frame length 3 during the inference stage in our experiments.

Secondly, we employ the joint training of the CTC and the CE losses. Given the feature sequence \mathbf{V} of a text line image, the text recognition task is to find the corresponding underlying n-character sequence $\mathbf{C} = \{\mathbf{C}_1, \mathbf{C}_2, \dots, \mathbf{C}_n\}$, i.e, compute the posterior probability $p(\mathbf{C}|\mathbf{V})$. The CTC can be regarded as a loss function of neural networks:

$$L_{\text{CTC}}(\Theta) = -\log\left(\sum_{\pi: \varphi(\pi)=\mathbf{C}} p(\pi|\mathbf{V}, \Theta)\right) \quad (10)$$

where Θ represents the parameters of the recognition network and π is the predicted character sequence under the constraint of $\varphi(\pi) = \mathbf{C}$. The function π only retains one of the consecutive adjacent repeating characters and removes the ‘blank’ characters. The CTC loss (Eq.10) can be efficiently computed by using the forward-backward algorithm [3]. For the auxiliary decoder in Fig. 5, the CE loss directly predicts the probability $p(C_t|\mathbf{x}_t)$:

$$L_{\text{CE}}(\Theta, \Gamma) = \prod_t p(C_t|\mathbf{x}_t) \quad (11)$$

Γ is the parameters of the decoder. Based on the feature sequence \mathbf{V} , the vector \mathbf{x}_t at the time step t can be computed using the following attention method:

$$\mathbf{q}_t = \tanh(\mathbf{W}_q \mathbf{h}_{t-1} + \mathbf{b}_q) \quad (12)$$

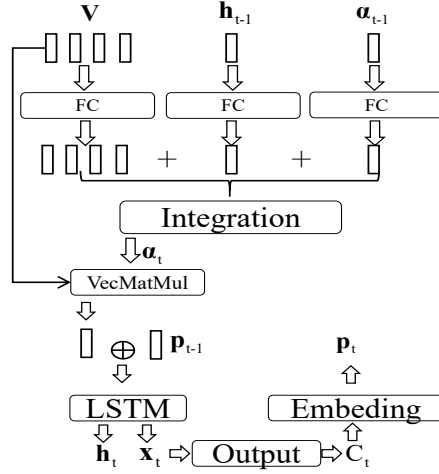


Fig. 5. The decoder with attention. The Integration is similar to the module in Fig. 3

$$\mathbf{k}_i = \tanh(\mathbf{W}_k \mathbf{v}_i + \mathbf{b}_k) \quad (13)$$

$$\mathbf{a}_t = \tanh(\mathbf{W}_a \mathbf{a}_{t-1}) \quad (14)$$

$$e_{t,i} = \mathbf{w}^T \tanh(\mathbf{q}_t + \mathbf{k}_i + \mathbf{a}_t) \quad (15)$$

$$\alpha_{t,i} = \frac{e_{t,i}}{\sum_i e_{t,i}} \quad (16)$$

$$\mathbf{x}_t = \text{LSTM}\left(\left(\sum_i \alpha_{t,i} \mathbf{v}_i\right) \oplus \mathbf{p}_{t-1}\right) \quad (17)$$

where $\mathbf{h}_{t-1}, \mathbf{p}_{t-1}$ are the hidden state of the LSTM and the decoded embedding vector at the time step $t-1$, respectively.

Finally, Alg.1 describes the joint training of the CTC and the CE Losses.

Algorithm 1 The joint training pipeline of the CTC and the CE losses.

Require:

The randomly initialized parameter sets $\{\Theta, \Gamma\}$;

The loss functions L_{CTC} , L_{CE} and the corresponding weight coefficients λ_1, λ_2 in the training stage of the main recognition network (MRN(Θ)), and the auxiliary decoder (Dec(Γ)), respectively.

1: Optimize the MRN parameter set Θ by using the Adam algorithm [30].

$\Theta = \text{Adam}(\Theta, L_{\text{CTC}})$

2: Jointly train the parameter set Θ, Γ based on the CTC and the CE losses.

$L = \lambda_1 L_{\text{CTC}} + \lambda_2 L_{\text{CE}}$

$\Theta, \Gamma = \text{Adam}(\Theta, \Gamma, L)$

3: **return** The MRN(Θ).

3 Experiments

3.1 Datasets and Evaluation Metrics

Table 1. The number of text lines, characters and classes in the SCUT-HCCDoc and the SCUT-EPT.

Type	SCUT-HCCDoc		SCUT-EPT	
	Training set	Test set	Training set	Test set
Text lines	93,254	23,484	40,000	10,000
Characters	925,200	230,019	1,018,432	248,730
Classes	5,922	4,435	4,058	3,236

The proposed network is validated on two Chinese handwritten text datasets(the SCUT-HCCDoc[31] and the SCUT-EPT[32]) and one English handwritten text dataset: the IAM[33].

All the images of SCUT-HCCDoc were obtained by Internet search. According to certain rules, only 12,253 images were preserved from the initial 100 thousand candidate images. These images were randomly split into the training and test sets with a ratio of 4:1. After splitting, the training set contains 9,801 images with 93,254 text instances and 925,200 characters. The test set contains 2,452 images with 23,484 text instances and 230,019 characters.

The Chinese handwritten text data set SCUT-EPT contains 4,250 categories of Chinese characters and symbols, totaling 1,267,162 characters, and it was split into 40,000 training text lines and 10,000 test text lines. These samples were collected from examination papers and were written by 2,986 students, and the training and test sets do not include the same writers. There are a total of 4,250 classes, but the number of classes in the training set is just 4,058. Therefore, some classes in the testing set do not appear in the training set and can not be correctly recognized.

Table 2. The standard partition of the dataset IAM.

Set name	Text lines	Writers
Train	6,161	283
Validation1	900	46
Validation2	940	43
Test	1,861	128
Total	9,862	500

For the English handwritten text recognition, we evaluate the performance of our method on the IAM dataset. The IAM dataset contains a total number of

9,862 text lines written by 500 writers. It provides one training set, one test set and two validation sets. The text lines of all data sets are mutually exclusive, thus, each writer has contributed to one set only.

Table 1 lists the number of text lines, characters and classes in both Chinese datasets. In the SCUT-EPT dataset, we removed 681 training text images including abnormal structures, i.e. characters swapping and overlap. Similarly, in the SCUT-HCCDoc dataset, some low-quality images were removed and only 91,261 text instances were used in the training set. All test images in both datasets were evaluated. Table 2 lists the standard partition of the English dataset ¹. All training images, validation images and test images were used in our experiments and the best model was selected for testing according to the results on the validation sets. The character accuracy rate (AR) was used to evaluate the performance of the text recognition model. The evaluation criterion is defined as follows:

$$1 - \frac{N_s + N_i + N_d}{N} \quad (18)$$

where N is the total number of samples in the evaluation set. N_s , N_i and N_d denote the number of substitution errors, insertion errors and deletion errors, respectively.

3.2 Experimental Results and Analysis

During the training stage, common data argument methods including text location shift, image blur, grey level and contrast changes, and linear transformation were used. The Adam optimization algorithm with default parameters was adopted, we adjusted the learning rate according to training steps until the model converged into a small range. At certain epochs, the learning rate was multiplied by 0.5. The deep learning platform Pytorch [34] and an NVIDIA RTX A6000 with 48GB memory were used. Firstly, we conducted ablation experiments to verify the effectiveness of the proposed network.

Ablation Experiments In this section, we examine several important factors for recognition performance. These factors include the frame resolution, the 3D attention module, the global-local context information and the multi-scale training.

We only compare the results of different frame lengths and all sliding windows have the same height. Table 3 shows the different results of different frame resolutions. We can observe that frame length 3 is the optimal configuration for all experiments, which means the corresponding window size is suitable for most characters. For a longer or shorter feature sequence, it is difficult to discriminate different regions of characters. For example, when we used a small frame length, the Chinese recognition results obviously decreased from 88.8% to 88.06%, 76.67% to 75.13%, respectively, while the English recognition performance only changed from 94.17% to 94.11%, which may be owing to a smaller

¹ <https://fki.tic.heia-fr.ch/databases/iam-handwriting-database>

width for most English characters. Furthermore, we can obtain consistently improvements by integrating multiple resolutions, i.e., the ARs achieve 89.16%, 76.96% and 94.37%, respectively. As shown in Fig. 2, in the training stage, although three 3D attention blocks and global-local context blocks were used in parallel, we only retained the corresponding branch of the frame length 3 during the inference stage.

Table 3. The different results of different frame resolutions.

Frame length	SCUT-HCCDoc	SCUT-EPT	IAM
2	88.06	75.13	94.11
3	88.8	76.67	94.17
4	87.21	76.36	93.62
Multi-scale	89.16	76.96	94.37

Based on the optimal frame length and single-scale training, Table 4 lists the results with/without the 3D attention module and the global-local context information. If we did not adopt the 3D attention module in experiments, a pooling operation was directly employed to reduce the height of the last convolutional feature maps to 1. The 3D attention module can steadily improve the Chinese recognition performances. On the SCUT-HCCDoc data set, the AR is improved from 88.51% to 88.8%. On the SCUT-EPT data set, the AR increases from 75.00% to 76.67%. Although it seems that the English recognition without the 3D attention module has a higher AR (94.31% vs. 94.17%), the network based on the multi-resolutions training still obtains the best AR. As the conclusions demonstrated by many previous researches, there exists an obvious gap with/without using the context information for the sequence task. The results dramatically decrease from 88.8% to 85.36%, 76.67% to 72.28% and 94.17% to 87.0%, respectively. It is interesting to observe that the pure CNN-based models without the 3D attention block and the context information can also achieve 85.76%, 72.53% and 85.93%, respectively.

Table 4. The recognition performance with/without different blocks.

3D attention module	Global-local context information	SCUT-HCCDoc	SCUT-EPT	IAM
✓	✓	88.8	76.67	94.17%
✓	✗	85.36	72.28	87.0%
✗	✓	88.51	75.00	94.31%
✗	✗	85.76	72.53	85.93

In Table 5, we compare the results of different training strategies, i.e. the weights are only optimized by the CTC loss or jointly trained by the CTC

loss and the CE loss. Although the Chinese decoding results of the auxiliary network are not good, the main recognition network still benefits from the joint training. The best network can achieve 89.34%, 77.15% and 94.41%, respectively. Moreover, we also list the storage and the running time comparisons of different methods. In order to make a fair comparison, all experiments were evaluated on the same machine and the experimental configurations on the same dataset were consistent. The decoding time of the CTC is defined as 1. Generally speaking, the results show that the ED method needs more time consumption and storage.

Table 5. The comparisons of accuracy rate, storage and relative speed.

Training strategy	SCUT-HCCDoc			SCUT-EPT			IAM		
	AR	Speed	Storage	AR	Speed	Storage	AR	Speed	Storage
CTC	89.16	1.0	41.92MB	76.67	1.0	35.62MB	94.37	1.0	22.04MB
CE	85.53	3.1	46.89MB	72.58	6.24	41.5MB	93.94	2.63	30.15MB
CTC + CE	89.34	1.0	41.92MB	77.15	1.0	35.62MB	94.41	1.0	22.04MB

Table 6. Performance comparison of our proposed method and other state-of-the-arts methods. For the English handwritten recognition task, all listed results do not use any lexicons.

Dataset	Method	Without external data	With external data
SCUT-HCCDoc	Zhang et al. [31]	78.65	79.84
	Peng et al. [25]	-	90.85
	Lin et al. [26]	-	88.10
	Ours	89.34	-
SCUT-EPT	Zhu et al. [32]	75.37	75.97
	Hoang et al. [7]	76.61	77.61
	Ngo et al. [12]	76.85	-
	Ours	77.15	-
IAM	Dutta et al.[6]	-	94.3%
	Chowdhury et al. [10]	91.9%	-
	Ours	94.41	-

Overall Comparison Finally, Table 6 shows an overall comparison of our proposed method and other state-of-the-art methods on different test sets. Without using external data, our proposed network can make a new milestone. Compared with the best networks trained by using external data, the proposed network can also keep comparable results on all datasets. For the listed results on the IAM

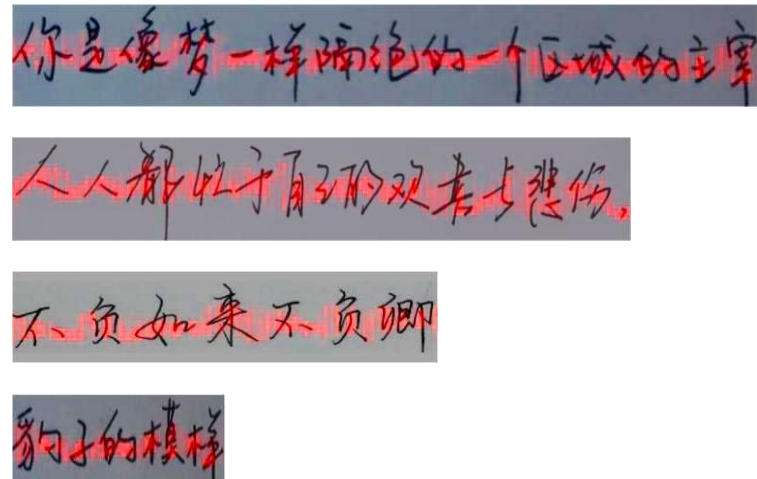


Fig. 6. The typical samples of the attention visualization on the SCUT-HCCDoc dataset.

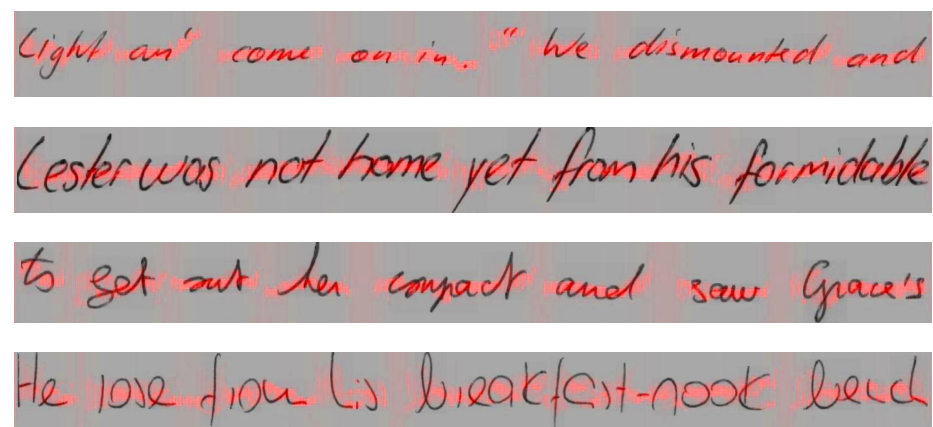


Fig. 7. The visualization of the 3D attention weights on the IAM images.

dataset, the standard partition and no word lexicons were used. Please note there exists an unofficial partition (RWTH partition) of the IAM dataset. It is widely used by many researchers, their results are not compared in this paper.

Visualization Analysis In Fig. 6, Fig. 7 and Fig. 8, the attention weights in the 3D block are shown on the original images. It is interesting to observe that even for long-text images and some small symbols, most attention weights (red parts) are still located on the handwriting characters, which demonstrates the proposed attention mechanism is reasonable.

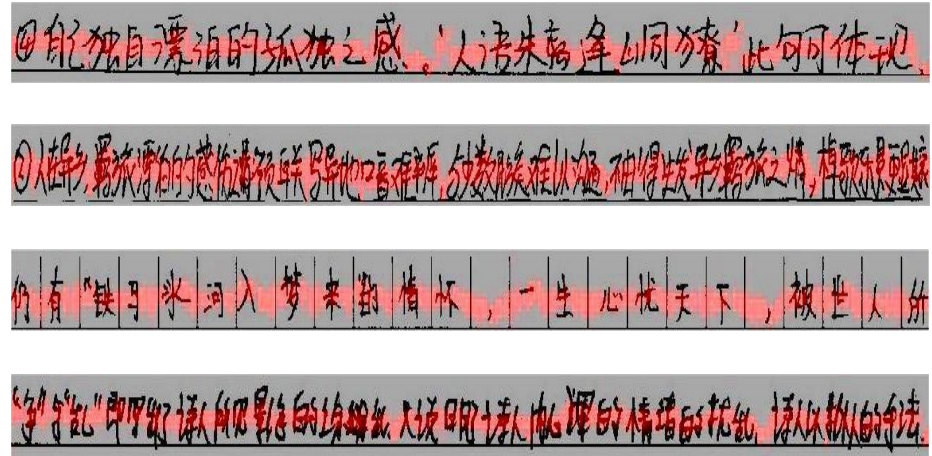


Fig. 8. The typical samples of the attention visualization on the SCUT-EPT dataset.

4 Conclusion

In this paper, main canonical neural units including attention mechanisms, fully-connected layer, recurrent unit and convolutional layer are ingeniously organized into a network. The network weights are effectively optimized by the multi-scale training. Experimental results show that the proposed method can achieve comparable results with the state-of-the-art methods. Besides, the visualization analysis demonstrates the proposed attention mechanism is reasonable. For future work, we will investigate large vision and language models for document analysis.

Acknowledgments

This work was supported by the National Natural Science Foundation of China under Grant No. 62106031. The author would like to thank Professor Jun Du of the University of Science and Technology of China (USTC). When the author was a Ph.D. candidate at USTC, we successfully applied the HMM and the deep neural network to the text recognition task. The supervisor (Prof. Jun Du) always said, can we combine three mainly segmentation-free methods? Although the HMM is not explicitly used in this paper, the question inspired the author to delve into this problem while self-isolated at home. The author also would like to thank Yan Wang for applying the code of extracting text lines from original SCUT-HCCDoc documents.

References

1. Salvador Espana-Boquera, Maria Jose Castro-Bleda, Jorge Gorbe-Moya, and Francisco Zamora-Martinez. Improving offline handwritten text recognition with hybrid

hmm/ann models. *IEEE transactions on pattern analysis and machine intelligence*, 33(4):767–779, 2010.

2. Zi-Rui Wang, Jun Du, and Jia-Ming Wang. Writer-aware cnn for parsimonious hmm-based offline handwritten chinese text recognition. *Pattern Recognition*, 100:107102, 2020.
3. Alex Graves, Santiago Fernández, Faustino Gomez, and Jürgen Schmidhuber. Connectionist temporal classification: labelling unsegmented sequence data with recurrent neural networks. In *Proceedings of the 23rd international conference on Machine learning*, pages 369–376, 2006.
4. Ronaldo Messina and Jerome Louradour. Segmentation-free handwritten chinese text recognition with lstm-rnn. In *2015 13th International conference on document analysis and recognition (icdar)*, pages 171–175. IEEE, 2015.
5. Baoguang Shi, Xiang Bai, and Cong Yao. An end-to-end trainable neural network for image-based sequence recognition and its application to scene text recognition. *IEEE transactions on pattern analysis and machine intelligence*, 39(11):2298–2304, 2016.
6. Kartik Dutta, Praveen Krishnan, Minesh Mathew, and CV Jawahar. Improving cnn-rnn hybrid networks for handwriting recognition. In *2018 16th international conference on frontiers in handwriting recognition (ICFHR)*, pages 80–85. IEEE, 2018.
7. Huu-Tin Hoang, Chun-Jen Peng, Hung Vinh Tran, Hung Le, and Huy Hoang Nguyen. lodenet: a holistic approach to offline handwritten chinese and japanese text line recognition. In *2020 25th International Conference on Pattern Recognition (ICPR)*, pages 4813–4820. IEEE, 2021.
8. Zi-Rui Wang and Jun Du. Fast writer adaptation with style extractor network for handwritten text recognition. *Neural Networks*, 147:42–52, 2022.
9. Dzmitry Bahdanau, Kyunghyun Cho, and Yoshua Bengio. Neural machine translation by jointly learning to align and translate. *arXiv preprint arXiv:1409.0473*, 2014.
10. Arindam Chowdhury and Lovekesh Vig. An efficient end-to-end neural model for handwritten text recognition. *arXiv preprint arXiv:1807.07965*, 2018.
11. Jianshu Zhang, Jun Du, and Lirong Dai. Radical analysis network for learning hierarchies of chinese characters. *Pattern Recognition*, 103:107305, 2020.
12. Trung Tan Ngo, Hung Tuan Nguyen, Nam Tuan Ly, and Masaki Nakagawa. Recurrent neural network transducer for japanese and chinese offline handwritten text recognition. In *International Conference on Document Analysis and Recognition*, pages 364–376. Springer, 2021.
13. Jiefeng Ma, Zirui Wang, and Jun Du. An open-source library of 2d-gmm-hmm based on kaldi toolkit and its application to handwritten chinese character recognition. In *Image and Graphics: 11th International Conference, ICIG 2021, Haikou, China, August 6–8, 2021, Proceedings, Part I* 11, pages 235–244. Springer, 2021.
14. Alex Graves and Jürgen Schmidhuber. Offline handwriting recognition with multidimensional recurrent neural networks. *Advances in neural information processing systems*, 21, 2008.
15. Joan Puigcerver. Are multidimensional recurrent layers really necessary for handwritten text recognition? In *2017 14th IAPR international conference on document analysis and recognition (ICDAR)*, volume 1, pages 67–72. IEEE, 2017.
16. Zhanzhan Cheng, Fan Bai, Yunlu Xu, Gang Zheng, Shiliang Pu, and Shuigeng Zhou. Focusing attention: Towards accurate text recognition in natural images. In *Proceedings of the IEEE international conference on computer vision*, pages 5076–5084, 2017.

17. Junyeop Lee, Sungrae Park, Jeonghun Baek, Seong Joon Oh, Seonghyeon Kim, and Hwalsuk Lee. On recognizing texts of arbitrary shapes with 2d self-attention. In *Proceedings of the IEEE/CVF Conference on Computer Vision and Pattern Recognition Workshops*, pages 546–547, 2020.
18. Haiyang Yu, Xiaocong Wang, Bin Li, and Xiangyang Xue. Chinese text recognition with a pre-trained clip-like model through image-ids aligning. In *Proceedings of the IEEE/CVF International Conference on Computer Vision*, pages 11943–11952, 2023.
19. Zhi Qiao, Yu Zhou, Dongbao Yang, Yucan Zhou, and Weiping Wang. Seed: Semantics enhanced encoder-decoder framework for scene text recognition. In *Proceedings of the IEEE/CVF conference on computer vision and pattern recognition*, pages 13528–13537, 2020.
20. Yuxin Wang, Hongtao Xie, Shancheng Fang, Jing Wang, Shenggao Zhu, and Yongdong Zhang. From two to one: A new scene text recognizer with visual language modeling network. In *Proceedings of the IEEE/CVF International Conference on Computer Vision*, pages 14194–14203, 2021.
21. Shancheng Fang, Hongtao Xie, Yuxin Wang, Zhendong Mao, and Yongdong Zhang. Read like humans: Autonomous, bidirectional and iterative language modeling for scene text recognition. In *Proceedings of the IEEE/CVF Conference on Computer Vision and Pattern Recognition*, pages 7098–7107, 2021.
22. Baoguang Shi, Mingkun Yang, Xinggang Wang, Pengyuan Lyu, Cong Yao, and Xiang Bai. Aster: An attentional scene text recognizer with flexible rectification. *IEEE transactions on pattern analysis and machine intelligence*, 41(9):2035–2048, 2018.
23. Denis Coquenet, Clément Chatelain, and Thierry Paquet. Dan: a segmentation-free document attention network for handwritten document recognition. *IEEE Transactions on Pattern Analysis and Machine Intelligence*, 2023.
24. Yew Lee Tan, Adams Wai-Kin Kong, and Jung-Jae Kim. Pure transformer with integrated experts for scene text recognition. In *European Conference on Computer Vision*, pages 481–497. Springer, 2022.
25. Dezhi Peng, Lianwen Jin, Weihong Ma, Canyu Xie, Hesuo Zhang, Shenggao Zhu, and Jing Li. Recognition of handwritten chinese text by segmentation: A segment-annotation-free approach. *IEEE Transactions on Multimedia*, 2022.
26. Weifeng Lin, Canyu Xie, Dezhi Peng, Jiapeng Wang, Lianwen Jin, Wei Ding, Cong Yao, and Mengchao He. Building a mobile text recognizer via truncated svd-based knowledge distillation-guided nas. 2023.
27. Dezhi Peng, Lianwen Jin, Yuliang Liu, Canjie Luo, and Songxuan Lai. Pagenet: Towards end-to-end weakly supervised page-level handwritten chinese text recognition. *International Journal of Computer Vision*, 130(11):2623–2645, 2022.
28. Sergey Ioffe and Christian Szegedy. Batch normalization: Accelerating deep network training by reducing internal covariate shift. In *International conference on machine learning*, pages 448–456. pmlr, 2015.
29. Ashish Vaswani, Noam Shazeer, Niki Parmar, Jakob Uszkoreit, Llion Jones, Aidan N Gomez, Łukasz Kaiser, and Illia Polosukhin. Attention is all you need. *Advances in neural information processing systems*, 30, 2017.
30. Diederik P Kingma and Jimmy Ba. Adam: A method for stochastic optimization. *arXiv preprint arXiv:1412.6980*, 2014.
31. Hesuo Zhang, Lingyu Liang, and Lianwen Jin. Scut-hccdoc: A new benchmark dataset of handwritten chinese text in unconstrained camera-captured documents. *Pattern Recognition*, 108:107559, 2020.

32. Yuanzhi Zhu, Zecheng Xie, Lianwen Jin, Xiaoxue Chen, Yaoxiong Huang, and Ming Zhang. Scut-upt: New dataset and benchmark for offline chinese text recognition in examination paper. *IEEE Access*, 7:370–382, 2018.
33. U-V Marti and Horst Bunke. The iam-database: an english sentence database for offline handwriting recognition. *International journal on document analysis and recognition*, 5:39–46, 2002.
34. Adam Paszke, Sam Gross, Francisco Massa, Adam Lerer, James Bradbury, Gregory Chanan, Trevor Killeen, Zeming Lin, Natalia Gimelshein, Luca Antiga, et al. Pytorch: An imperative style, high-performance deep learning library. *Advances in neural information processing systems*, 32, 2019.